SSCL-559

SSCL-559

Superconducting Super Collider Laboratory

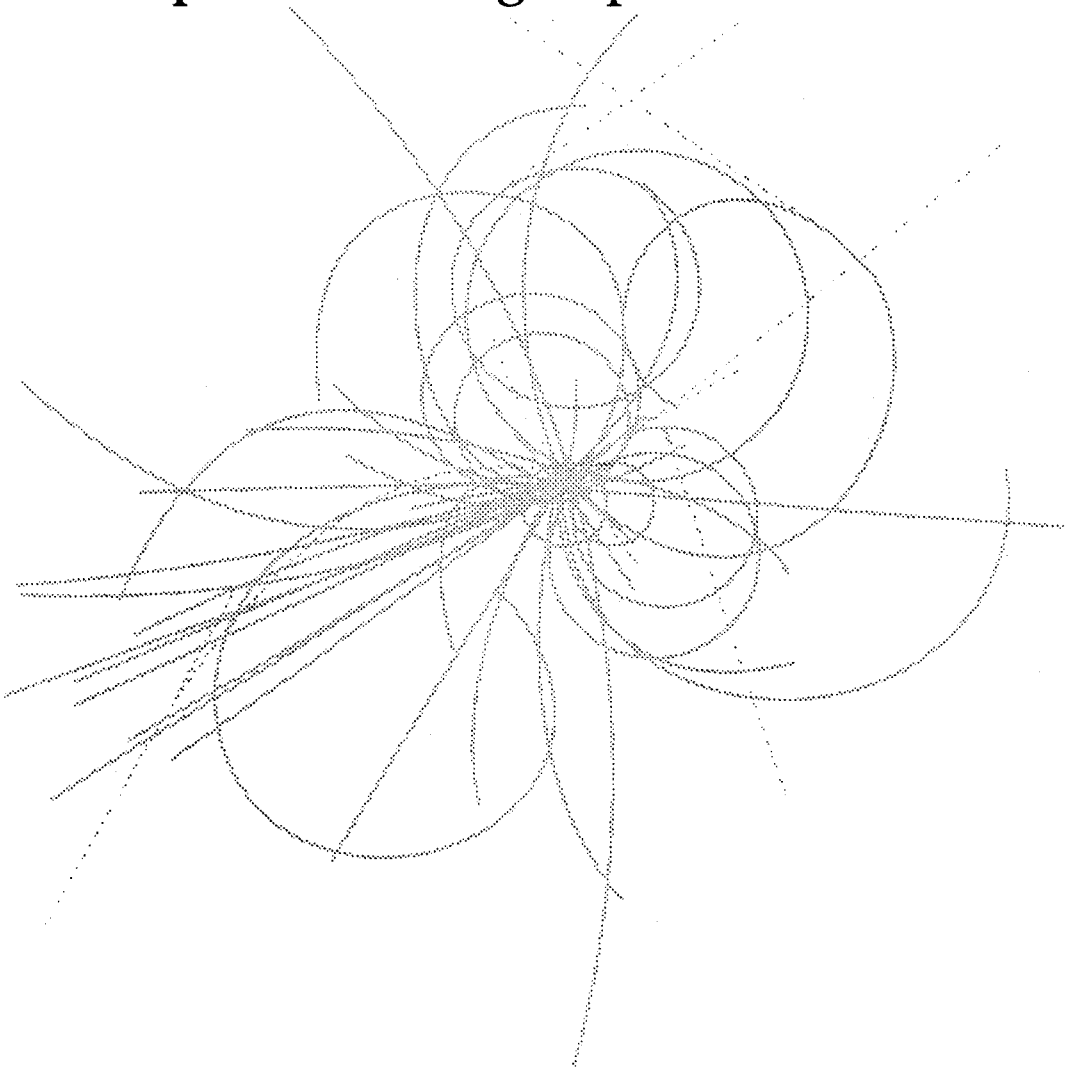

Beam Control Feedback Loops for the Low Energy Booster

L. K. Mestha

October 1991

SSCL-559

Beam Control Feedback Loops for the Low Energy Booster

L. K. Mestha

Accelerator Systems Division
Superconducting Super Collider Laboratory†
2550 Beckleymeade Ave.
Dallas, TX 75237

October 1991

†Operated by the Universities Research Association, Inc., for the U.S. Department of Energy under Contract No. DE-AC35-89ER40486.

CONTENTS

FIGURES iv

1.0 INTRODUCTION 1

2.0 FEEDBACK LOOPS LOCAL TO THE RF CAVITY 1

2.1 Local Phase and Amplitude Loop 3

2.2 Cavity Tuning Loop 3

3.0 FEEDBACK LOOPS GLOBAL TO THE RF CAVITY 7

3.1 Global Frequency and Phase Control Loops 7

3.2 Global Amplitude Control Loops 10

3.3 Global Paraphasing Control Loops 10

REFERENCES 11

FIGURES

1 Equivalent Circuit of the Cavity 1

2 Phasor diagram representing the beam current, generator current, cavity voltage, and tuning angle with perturbed quantities 2

3 Local Phase and Amplitude Loops 4

4 Cavity Tuning Loop 4

5(a) Cavity Q (theoretical) with respect to frequency 5

5(b) Allowable frequency shift with respect to rf for a maximum detuning angle of 10°. 5

6(a) Rate of change of frequency with respect to current of the tuner power supply 6

6(b) Variation of expected frequency shift with respect to LEB cycle time when all the global loops are closed. 6

6(c) First derivative of Figure 6(b) with respect to time 7

7 Schematic representation of Beam Control Feedback Loops for the LEB. 9

8 LEB Trip-plan. 10

1.0 INTRODUCTION

There are several feedback loops associated with a basic low-level rf system for the Low Energy Booster (LEB) of the Superconducting Super Collider. The goal of the system is to be able to bunch the beam, accelerate it, and extract it to the Medium Energy Booster (MEB). A precise control of the frequency, phase, and amplitude of the cavity gap voltage is required. Although, the number of parameters to be ultimately controlled does not appear to be high, in practice controlling them is complicated. Hence we have made an effort here to outline all the necessary feedback loops, including those being used for the cavity. Requirements and design goals for some of them are highlighted.

2.0 FEEDBACK LOOPS LOCAL TO THE RF CAVITY

We can imagine three feedback loops local to the cavity: a cavity tuning loop, a local phase loop, and a local amplitude loop. High-bandwidth local phase and amplitude loops are required to minimize the power loss in the tube and to maintain the voltage as seen by the beam in order to minimize the change in bucket area with the beam going through the cavity. We can understand the requirements of these loops by considering a simple equivalent circuit of the resonant system. The impedance of the equivalent circuit shown in Figure 1 is given by:

$$Z = \frac{R}{1 + iQ\left(\frac{\omega_R}{\omega_{RF}} - \frac{\omega_{RF}}{\omega_R}\right)}, \tag{1}$$

where ω_R is the resonant frequency and ω_{RF} is the RF frequency.

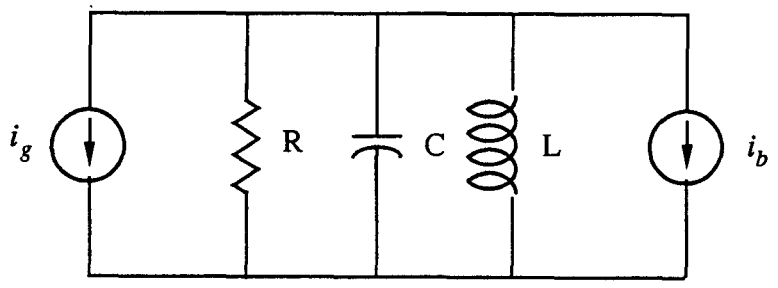

Figure 1. Equivalent Circuit of the Cavity.

If the detuning angle is represented by the equation below:

$$\tan\phi_y = \frac{2Q(\omega_R - \omega_{RF})}{\omega_R}, \tag{2}$$

then the impedance can be rewritten in the following form:

$$Z = \hat{R}e^{i\phi_y}, \tag{3}$$

where $\hat{R} = \frac{R}{\sec\phi_y}$. Hence the voltage on the gap is given by

$$V = \hat{R} I_t e^{i\phi_y} \quad , \tag{4}$$

where $I_t = I_b + I_g$, the sum of the rms values of the beam current and the generator current. A phasor diagram of the beam current, I_b, the generator current, I_g, and the cavity voltage, V, are shown in Figure 2, with the tuning angle, ϕ_y, at a given instance of time.

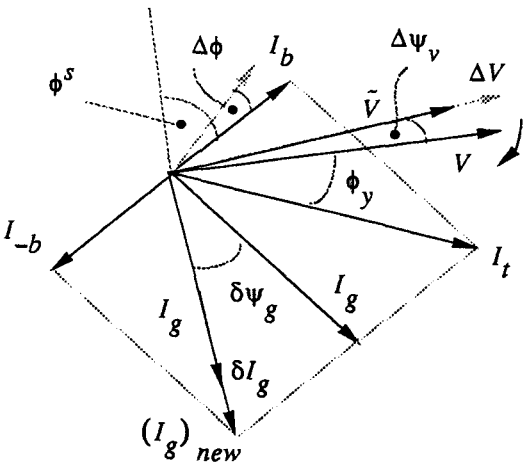

Figure 2. Phasor diagram representing the beam current, generator current, cavity voltage, and tuning angle with perturbed quantities.

In the above phasor diagram, perturbation in the phase and in the magnitude of the voltage is shown by $\Delta\psi_v$ and ΔV, respectively. The beam phase is shown perturbed by $\Delta\phi$ from the synchronous phase, ϕ^s, due to the dipole field error. When the tuning angle, ϕ_y, is zero the system is on tune. Under this condition the vector sum of the generator current and the beam current as seen by the cavity is in phase with the cavity voltage. Hence the power loss in the tube due to beam-loading is very high. To reduce the power loss due to beam-loading and to maintain the cavity voltage to a desired value, any or all of the following four steps can be taken:

1. Shift the phase of the generator current by an amount $\delta\psi_g$. This is done by the local phase loop by measuring $\Delta\psi_v$ and shifting the phase of the input signal to the power amplifier.
2. Increase the amplitude of the generator current by δI_g. This is done by the local amplitude loop by measuring ΔV and modulating the amplitude of the generator current by an amount, δI_g.

3. Add a beam current, I_{-b}, opposite in phase to the real beam current, I_b. This is done by adding a current program to the RF signal at 90° to the generator current at the input end of the power amplifier from an inexorable program.
4. Detune the cavity by an angle $\phi_y = \text{atan}\,(I_b/I_g)$. This is done by the cavity-tuning loop by measuring the tuning phase, ϕ_y, and modulating the bias regulator current driving the ferrite tuner.

By following these steps we would in effect be able to rotate the voltage vector theoretically to coincide with the generator current. This will be the desired optimum condition for the power tube. From the beam point of view, we need to have the perturbed voltage, ΔV, made equal to zero so that the bucket area is maintained at the desired value. From Eq. 4 it is clear that the proper variation in the magnitude of the total current, I_t, and the tuning angle, ϕ_y, will in fact show the desired change in the cavity voltage. The detuning of the cavity cannot be done as fast as the other three steps indicated above due to a large time constant involved in the ferrite tuner. In practice, there are, however, a fast-phase and amplitude loop and a low-bandwidth tuning loop. The perturbed beam phase from the synchronous phase due to field error is controlled globally in the global phase loop. We describe conceptually these feedback loops below.

2.1. Local Phase and Amplitude Loop

The local phase loop in essence consists of a phase detector, PD_1^P, a feedback controller, and a phase shifter, PS_1^P, as shown in Figure 3. The phase detector measures the phase difference between the rf signal supplied from the global frequency control unit and the measured gap voltage. The phase loop operates by changing the phase of the generator current at the rf signal frequency driving the power amplifier. It is required to account for the fixed-phase difference due to propagation delay across the power amplifier and the cavity. The phase loop is included with a set point summing node, SN_1^P, to vary the phase from a programmed signal. This facility is required while doing the paraphasing of the cavities at the beginning or end of the LEB cycle. We describe the paraphasing aspects of the system later in this report. The local amplitude loop shown in Figure 3 changes the amplitude of the generator current. It is planned at this stage to measure the amplitude envelope of the gap voltage and to compare it with a reference voltage signal to produce an amplitude error signal, δV_1, at the summing node point, SN_1^V. This signal is processed in a feedback controller at 1 MHz rate to produce appropriate amplitude modulation, δI_g, on the generator current.

2.2. Cavity Tuning Loop

Each cavity is required to operate within a certain tuning range. The phase detector, PD_1^T, measures the phase difference between the cavity gap voltage and the output of the power amplifier. This signal is fed to the bias regulator through a controller driving the ferrite tuner to correct for the tuning error (see Figure 4). A function generator, FG_1^T, is included in the system, if it is desirable to have a pre-programmed profile for the bias regulator. When the tuning is perfect, the phase measured from the phase detector, PD_1^T, should be equal to the phase shift due to the propagation delay across the cavity. Different controllers should be tried to improve the quality of the tuning feedback.

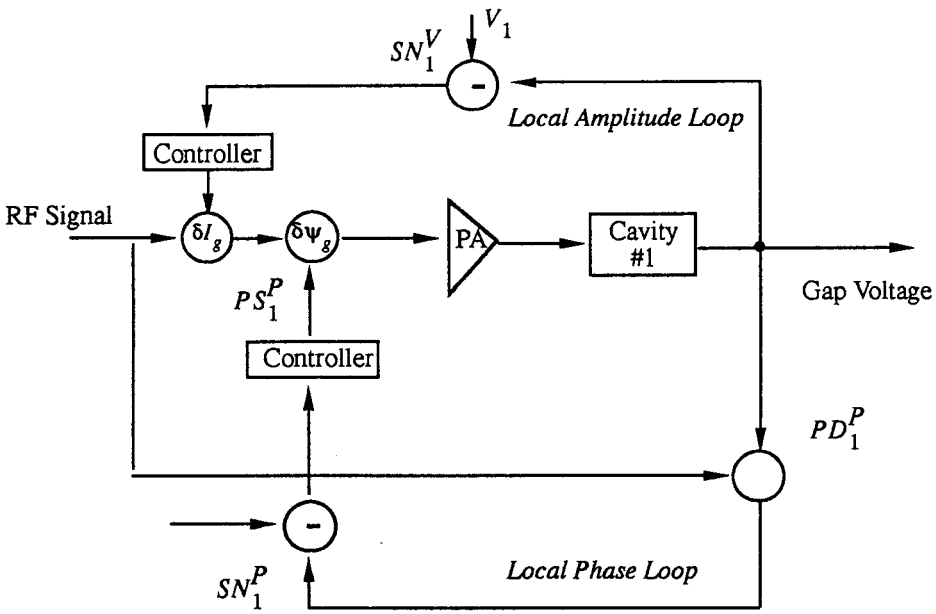

Figure 3. Local Phase and Amplitude Loops.

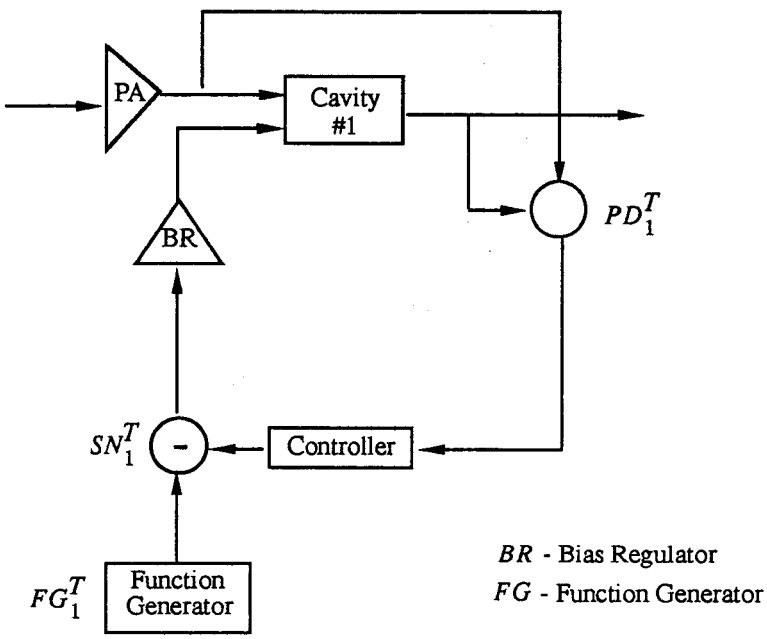

Figure 4. Cavity Tuning Loop.

There are several parameters required to design the tuning loop. They influence the interaction of the tuning loop with the other loops in the system. For example, if we restrict our tuning angle, ϕ_y, not to swing above 10°, then for a cavity with $Q = 5000$ and a resonant frequency of 50 MHz, the frequency of the rf signal driving the power amplifier must be within 882 Hz, calculated from the Robinson stability criteria shown in Eq. 2. In Figure 5(a) the plot of the cavity Q is shown. In Figure 5(b) the maximum detuning frequency is shown with respect to rf frequency for the whole LEB cycle.

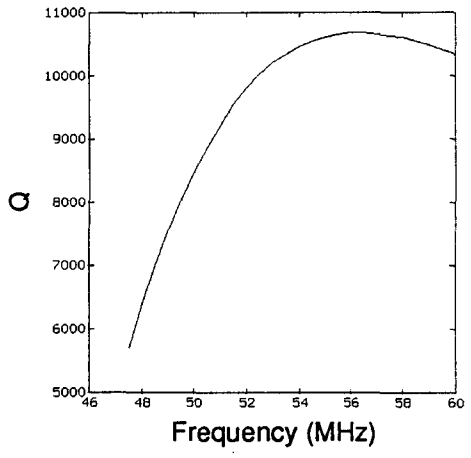

Figure 5(a). Cavity Q (theoretical) with respect to frequency.

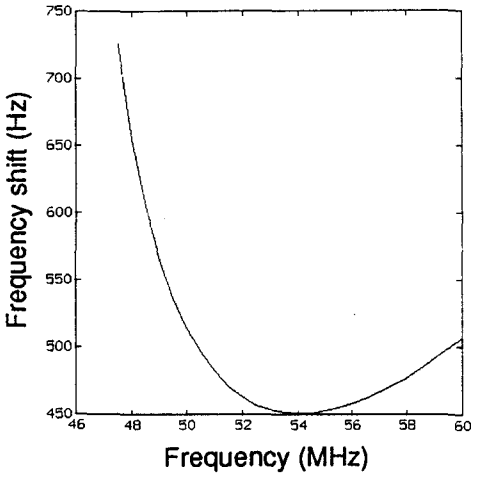

Figure 5(b). Allowable frequency shift with respect to rf for a maximum detuning angle of 10°.

The other factor influencing the design of the tuning system is the rate at which the frequency of the rf signal is changing with respect to time. If the function generator, FG_1^T, is producing a tuning profile to track the synchronous particle, then the rate at which the frequency shift supplied by the global feedback loops to the power amplifiers must be considered. This frequency shift, δf, can be expressed by the following relationship:

$$\frac{d\delta f}{dt} = \frac{\Delta V}{L}\frac{d\delta f}{di} \quad , \tag{6}$$

where ΔV is the over-voltage allowable on the bias regulator on top of the nominal value needed to maintain the tuning profile demanded by the function in the function generator, L is the inductance of the ferrite tuner, and $(d\delta f)/(di)$ is the scaling factor of the bias regulator as shown in Figure 6(a). Clearly, once the inductance and the scaling factors are fixed, the rate of frequency can be increased by increasing the over-voltage rating on the bias regulator. The maximum rate of frequency shift above the nominal frequency depends on various global feedback loops. In Figure 6(b) and 6(c) we show the variation of these values with respect to the LEB cycle while tracking a single particle in the LEB injected at 40° initial phase, with expected random errors in the dipole field, amplitude of the cavity voltage, radial orbit measurement, and the synchronization loop. We used the single-particle tracking code shown in Reference 1. On top of the quantities described above we need to know the accuracy with which the

minimum B-field is detected, since the starting point for the synchronous frequency curve depends on this. However, an inaccuracy of 20 μs would give about 20-KHz frequency offset from the programmed tuning curve. This is unacceptable due to a very high Q tuning system. Alternatively, *a priori* frequency information from the global frequency control system to the tuning system as a feed-forward loop can minimize the danger. Presently, such a feed-forward system has been evaluated and will be documented in a separate report.

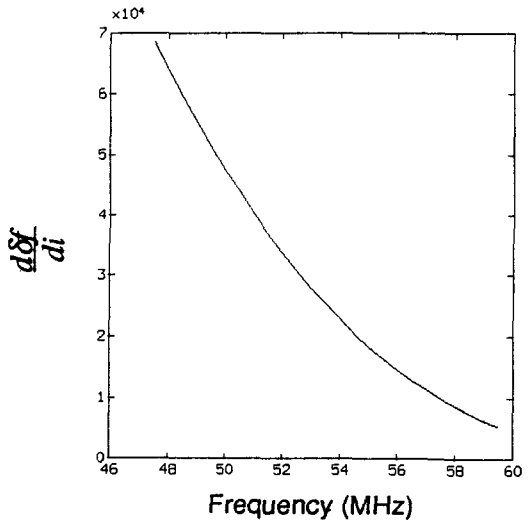

Figure 6(a). Rate of change of frequency with respect to current of the tuner power supply.

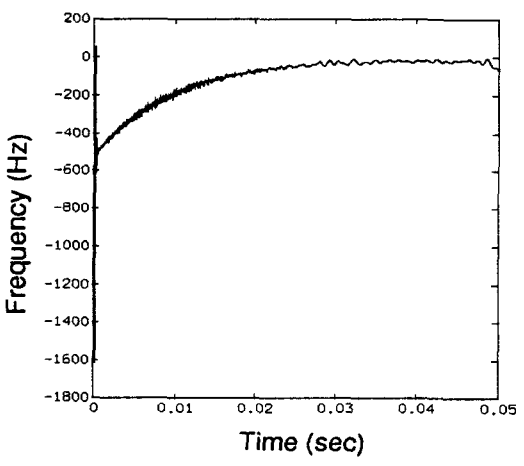

Figure 6(b). Variation of expected frequency shift with respect to LEB cycle time when all the global loops are closed.

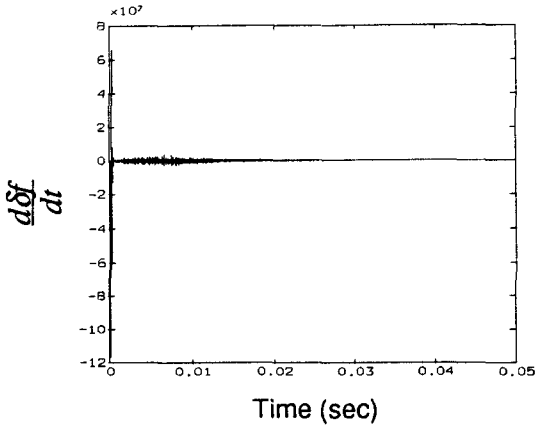

Figure 6(c). First derivative of Figure 6(b) with respect to time.

3.0 FEEDBACK LOOPS GLOBAL TO THE RF CAVITY

The global feedback loops have the special tasks of controlling the beam to capture and accelerate while correcting for radial excursions due to field errors, and ultimately of synchronizing the beam with the MEB reference bucket. The sequencing of LEB cycles to fill the collider rings is an additional requirement. Figure 7 shows a schematic diagram of the combined global and local feedback loops. The local cavity feedback loops are shown with an additional direct rf feedback loop, which minimizes the coupling effects between the local amplitude and phase loop. The global loops are divided based on their functionality and are generally centered around the frequency source. They are (1) Radial Loop, (2) Beam Phase Loop, and (3) Synchronization Loop. The interconnection of these loops as shown in this figure, however, is not optimal either in terms of implementation or of performance. At this stage we are investigating this feature, and some useful design techniques are shown in Reference 2.

3.1 Global Frequency and Phase Control Loops

The configuration we have presented looks very similar to that used for the Fermilab Booster. The heart of the system includes a Direct Digital Synthesizer (DDS) producing a sinusoidal rf signal by way of reading frequency values from a table. The table is stored with a ramping frequency profile, which is calculated from the ideal magnetic-field curve. All the corrections are added to the input or output of the DDS. The phase corrections to the rf signal are done using a radial loop. The radial position of the beam is measured with a horizontal electrode of the beam position monitor. The signal is digitized using a 10- or 12-bit Analogue to Digital Converter (ADC) and is read into a Digital Signal Processor (DSP). If the least significant bit represents a 0.1-mm accuracy, then an 8-bit ADC will read a maximum radial excursion of ±1.28 cms, whereas a 10-bit ADC can give sufficient maximum value. The radial position values are compared with the desired δR program stored in the signal processor. Radial position steering capability is required to deliberately move the transverse orbit, sometimes for studies related to machine physics. The resulting radial position value is processed through a feedback controller, then converted to analogue signal using a Digital to Analogue Converter (DAC). The phase shift is done by a good resolution analogue phase shifter, *PS*.

In the beam phase loop, the beam position signal is compared directly from a wall current monitor (without any pre-processing, as in the radial loop) in a beam phase detector, *BPD*, with the signal from the probe measuring the gap voltage. It is then digitized using a 12-bit ADC and is read into the DSP. The 12-bit ADC can give as much as 22 millidegrees resolution, since we are interested in a maximum phase of 90° only. The measured phase values are compared with the stored synchronous phase values, ϕ^S. The beam phase error is then converted to appropriate frequency shift through a feedback controller. The frequency shift is added to the ideal values in the adder circuits at the input end of the DDS. If there is systematic error in the beam phase loop, then the error will appear in the radial loop. Hence the radial loop will act against this systematic error and compensate for it, thus maintaining the beam on orbit. The beam phase loop may need to operate at a frequency at least 10 times that of the maximum synchrotron frequency to damp the oscillations due to dipole field error. At this stage we think the hardware we have chosen is capable of reaching a speed of 500 KHz.

The synchronization loop is configured depending on the approach one can adopt in achieving synchronization. If we use the "trip-plan" approach (as in Reference 3), then a Time to Digital Converter (TDC) is used to measure the position of the designated LEB reference signal for each MEB revolution. This time-of-flight information is read into a DSP and is then converted to position using the stored velocity profile for the synchronous particle. It is then compared with the ideal values for each MEB revolution, called the trip-plan. The resulting error is converted to frequency shift by passing through a feedback controller. The frequency shift from the controller is fed to the adder circuits at the input to the DDS. In this way we can enable the synchronization loop to follow the pre-programmed trip-plan. In Figure 8 we show a trip-plan for the new LEB with the rf parameters shown in Reference 1. The trip-plan shown in this figure is the modulo of the LEB circumference for each MEB turn. If there is a need for higher sampling, i.e., for having the trip-plan calculated twice every MEB turn, then the limitation is on the processing time in the DSP, and the time involved in the phase measurement. This may not seem to be a major concern due to the slow time constant involved in the synchronization loop. If we use a feed-forward loop from the δR measurement, then we would not need the radial loop for normal operation.

The hardware in the synchronization loop would include a phase detector if we decide to choose a phase-slippage scheme instead of the trip-plan approach. In the phase-slippage scheme the DDS is allowed to sweep with about 1-KHz frequency offset as compared to the MEB injection frequency. The phase detector will give the phase difference between two designated reference rf waves. Due to the frequency shift that we have deliberately introduced into the LEB DDS, there will be a beat point at a 1-ms interval between the LEB and MEB reference waves. We detect these points using a phase detector, then we invoke transfer. This scheme will not provide the means to pick up a given LEB reference wave and to lock the MEB rf. If we use a phase-locking approach as in the Fermilab Booster, then we need to close the synchronization loop a few milliseconds before the flat B-field region. A phase detector will be used instead of a TDC to measure the phase information between the LEB and the MEB reference waves. The phase values are compared with a table to follow a smooth program upto the extraction frequency by adding frequency shift to the adder circuits. A reliable and highly stable DDS is required to implement this technique. Otherwise, an alternative frequency source is required to make the phase difference zero.

We have derived a non-linear beam control model to analyze the global feedback loops. A good theoretical insight is required to understand why some of the loops are needed and how to optimize them. The stability limits are another concern in the feedback loops. For more details on these issues, the reader is advised to consult Reference 2.

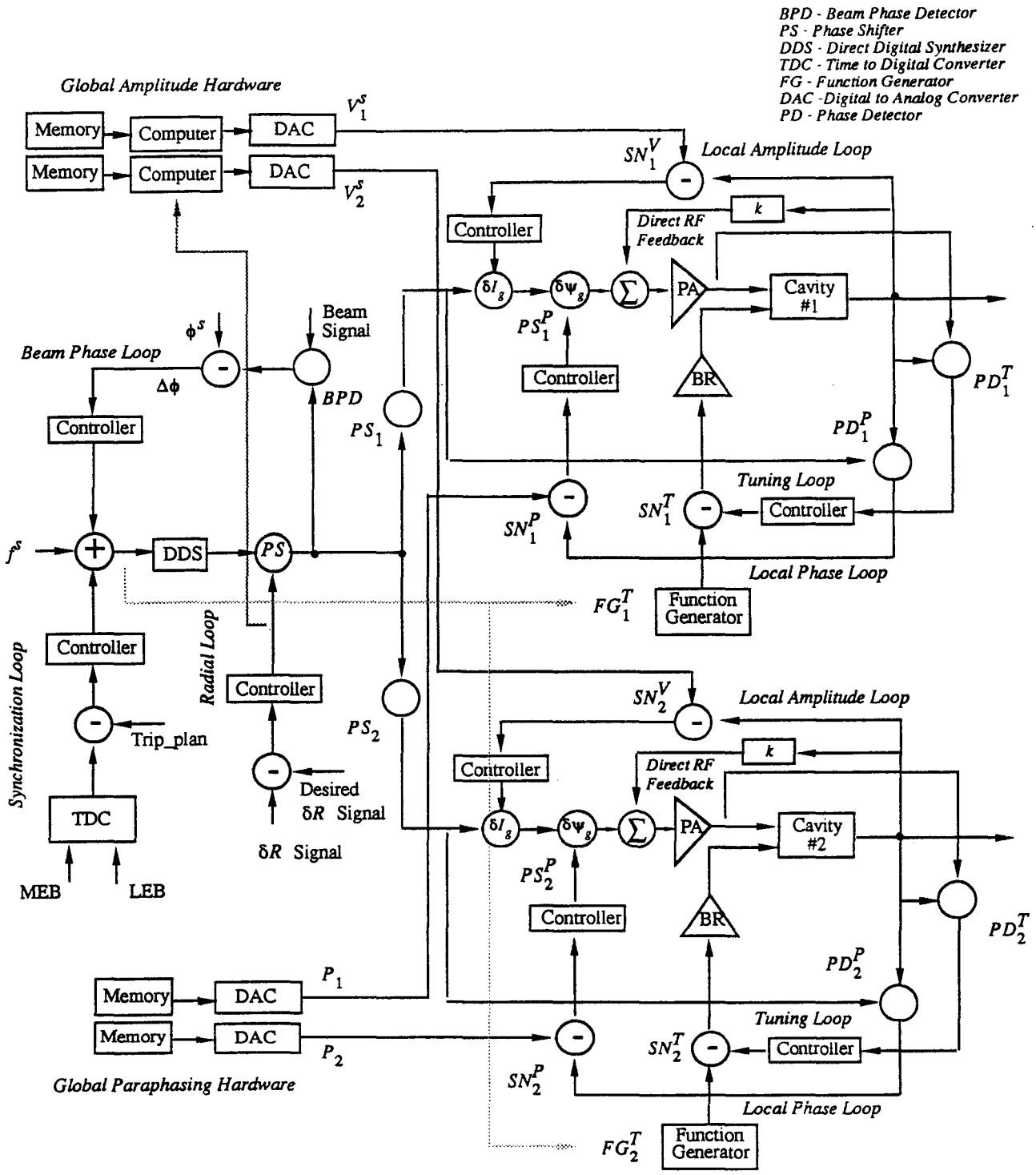

Figure 7. Schematic representation of Beam Control Feedback Loops for the LEB.

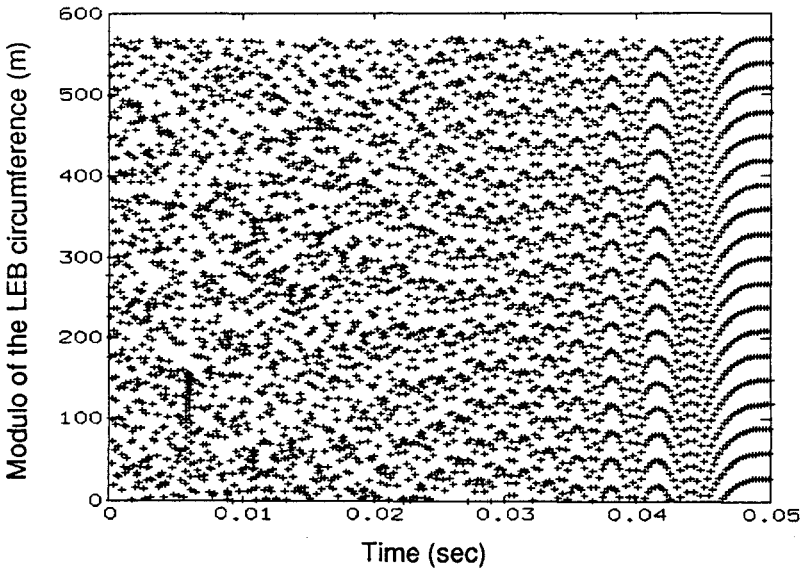

Figure 8. LEB Trip-plan.

3.2 Global Amplitude Control Loops

The global amplitude loops shown in Figure 7 have the hardware to generate signal representing the programmed amplitude curve for the whole LEB cycle to each cavity. Schematically, a Memory-Computer-DAC configuration is more suitable than a function generator. If the maximum output of DAC is 10 V representing 100 kV on the cavity, then 2.44 mV corresponds to a resolution of 24.4 V on the gap. The computer would help to include a digital feedback loop to the global amplitude from the radial position or the beam phase signal. On the contrary, an analogue global amplitude loop is subjected to noise in the amplitude due to large dynamic range. The global beam control model shown in Reference 2 gives a good indication about why this would be helpful. We have also obtained a stability criterion from the coupled beam control model when the rest of the global loops are closed. To achieve good control over the amplitude, the beam model shows that the measurement of global ring voltage is not necessary. Also, when we do this, it would be possible to update the function in the tuner loop function generator by reading the frequency values going to the DDS. Especially by using the DDS, we can rely on the frequency values up to a resolution of 0.2 Hz or more in the 47–60 MHz range.

3.3 Global Paraphasing Control Loops

The set point summing nodes, SN_1^P and SN_2^P, are being used to connect the paraphasing signals to the cavities. The hardware simply includes memory and a DAC. For a maximum of 180° phase shift in the gap voltage of cavity #2 with respect to the gap voltage of cavity #1, an 8-bit DAC will give a resolution of 0.7°. Also, the change with respect to time is another factor to determine the speed of the digital hardware. At this stage, we do not know how many cavities are involved in paraphasing. A feedback loop from any of the global parameters to the paraphasing hardware is not being considered. The rate of change of the cavity phase during paraphasing is another deciding factor in the selection of hardware. Mathematically, this is quite involved and hence is not included in this report.

REFERENCES

1. L.K. Mestha, *Particle Tracking Code for Simulating Global RF Feedback*, SSCL Report SSCL-506, 1991.
2. L.K. Mestha, C.M. Kwan, and K.S. Yeung, "Instabilities in Beam Control Feedback Loops in Proton Synchrotrons," to be published in *Journal of Particle Accelerators*.
3. L.K. Mestha, "Phase-Locked Loop With Controlled Phase Slippage," U.S. Patent application, DOE Case No. S-74, 282.